

# Active Roll Control Strategy using Fuzzy Logic Control Active Suspension

AMRIK SINGH PHUMAN SINGH, INTAN ZAURAH MAT DARUS

Advanced Vehicle Technology Research Group

Centre for Advanced Research on Energy

Universiti Teknikal Malaysia Melaka

Hang Tuah Jaya, 76100 Durian Tunggal, Melaka

MALAYSIA

Department of Applied Mechanics

Faculty of Mechanical Engineering

Universiti Teknologi Malaysia

81310 Skudai, Johor Bahru

MALAYSIA

amriksingh@utem.edu.my, intan@fkm.utm.my

*Abstract:* - An active roll control system using a combination of feedback and feedforward fuzzy logic control active suspension for enhancement of vehicle roll dynamics is presented in this paper. The dynamics model representing the vehicle behavior was first developed and then modeled in the Matlab/SIMULINK environment. The tire model used was developed based on tire test data using loop up table method. The validity of the vehicle model was verified using CarSim software for double lane change maneuver. The inputs to the feedforward fuzzy logic control were the driver steering wheel angle and vehicle longitudinal velocity and the output of the feedforward fuzzy logic control was the counter roll moment. For the feedback fuzzy logic control, the roll angle error and error rate were the inputs whereas the counter roll moment was the output. The effectiveness of the proposed control system was demonstrated for fishhook, step steer, and double lane change maneuvers and this vehicle roll control system has shown its capability in reducing vehicle rollover propensity.

*Key-Words:* - Active roll control, Rollover, Fishhook, CarSim, Fuzzy logic control;

## 1 Introduction

Among the types of crashes, rollover is one of a most dangerous crash due to the relatively high number fatalities. Although only 3% of the accidents lead to vehicle rollover, vehicle rollover is the contributing factor to 33% of all the fatalities [1]. High center of gravity vehicles such sport utility vehicles (SUV) are more likely to rollover compared to vehicles with a lower center of gravity height. According to the rollover resistance rating by NCAP, SUVs have an average of 3 star rating due to its high center of gravity location. In general, vehicle rollover may be divided to tripped and untripped rollover. Tripped rollover happens when the vehicle slips laterally of the road and comes into contact with obstacles such as curb and guardrail or the wheel, hitting a pot hole which yields a roll moment that causes the vehicle to rollover. In contrast, untripped rollover occurs on the road under extensive driver inputs such as negotiating a tight corner with high vehicle velocity. The rollover avoidance system can be realized through the rollover warning system and active roll control. The

rollover warning system is a passive system in which warning is given to alert the driver so that the driver can take corrective action by reducing the steering angle or vehicle speed to avoid rollover. Among the rollover warning system that can be found in literature are early warning safety device [2], dynamic rollover threshold [3] and time to rollover metric [4]. In active roll control, the vehicle detects the possibility of rollover and vehicle itself takes the corrective action to avoid rollover without requiring any input from the driver. The active roll control can be divided based on the types of actuation. The types of actuation are active suspension [5,6], active roll bar [7], differential braking [8,9], and active steering [10,11]. It is important that the vehicle roll motion is reduced to avoid rollover possibility and hence increase the safety of the vehicle user. There is possibility that the vehicle rollover can be recovered if the driver is skillful enough but it is more than impossible for a typical driver to avoid rollover when the vehicle is at its handling limits.

In this paper, a combination of feedforward and feedback fuzzy logic control using active suspension is implemented on a vehicle dynamics model to reduce the roll motion of the vehicle. The remaining of the paper is organized as follows: a 14 DOF vehicle model coupled with look up table tire model is presented in Section 2. Section 3 presents the active roll control structure which consists of feedforward and feedback fuzzy logic control schemes. The simulation results are presented in Section 4. Finally, the conclusion of the study is made in Section 5.

**2 Vehicle Modeling**

In literature, there are various vehicle models are employed in the implementation of the vehicle control strategies such as traction control, active braking, suspension control, and vehicle stability control. The vehicle models developed should be simple enough for the purpose of control system design, but at the same time having the capability represent the important aspects of the dynamics. In this paper, a full vehicle model with look up table tire model is developed for the purpose of predicting the dynamic behavior of the vehicle. The vehicle model presented in this paper is extensively used by researchers as a tool to investigate and enhance vehicle handling. The vehicle model as shown in Fig. 1 is made up of six degrees of freedom at the vehicle center of gravity and two degrees of freedom at each unsprung mass. Longitudinal, lateral, vertical, roll, pitch, and yaw are the motions at the vehicle center of gravity. The motions of the unsprung mass are the wheel vertical travel and wheel spin. Similar full car vehicle models can be found in literature [5,12].

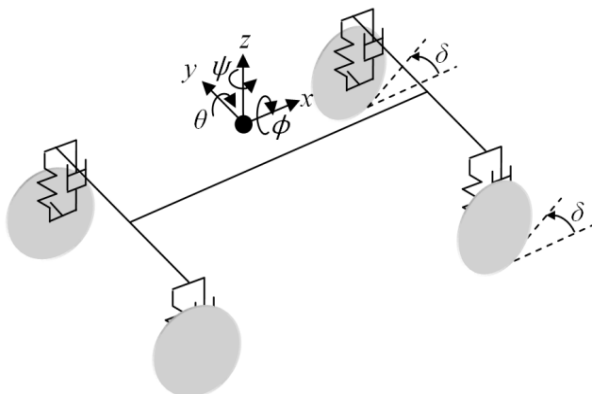


Fig. 1. 14 DOF vehicle model

**2.1 Vehicle Modelling Assumptions**

In order to simplify the complexity of the actual vehicle, a few assumptions were made to develop the vehicle dynamics model. The steering wheel angles for the front left and right wheels were

assumed to be the same. The wheel maintains contact with the road throughout the maneuvers and both wheel and suspension stay normal to the ground. The longitudinal and lateral tire behaviors are represented by the nonlinear table whereby the longitudinal force is a function of slip ratio and normal load and the lateral force is a function of tire slip angle and normal load. Vertical tire behavior is represented by equivalent spring stiffness. Small angles are considered for the vehicle roll, pitch, and yaw angles to avoid the need for coordinate transformation. Suspension spring and damper have linear properties.

**2.2 Equations of Motion for 14 DOF Vehicle Model**

The Fig. 2 shows the vehicle handling model which includes the motion along the longitudinal axis, lateral axis, and rotation about the vertical axis.  $F_{xij}$  and  $F_{yij}$  are the longitudinal and lateral tire forces respectively. The subscript  $i$  denotes front ( $f$ ) or rear ( $r$ ) whereas the subscript  $j$  represents left ( $l$ ) or right ( $r$ ).

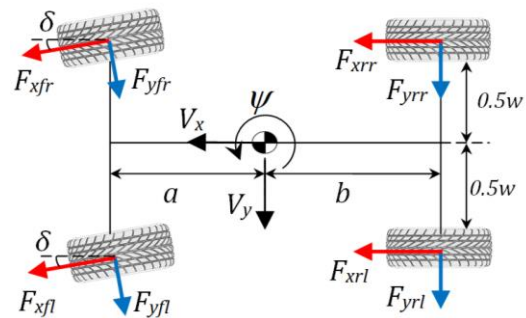


Fig. 2. Vehicle handling model

By applying Newton’s Second Law of Motion, the equation of motion along the longitudinal direction is given as

$$F_{xfl} \cos \delta - F_{yfl} \sin \delta + F_{xfr} \cos \delta - F_{yfr} \sin \delta + F_{xrl} + F_{xrr} = m(\dot{V}_x - V_y \dot{\psi} + \dot{Z}_s \dot{\theta}) \tag{1}$$

The lateral equation of motion can be written as

$$F_{xfl} \sin \delta + F_{yfl} \cos \delta + F_{xfr} \sin \delta + F_{yfr} \sin \delta + F_{yrl} + F_{yrr} = m(\dot{V}_y + V_x \dot{\psi} - \dot{Z}_s \dot{\phi}) \tag{2}$$

The following is the equation of motion for the yaw motion

$$aF_{xfl} \sin \delta - \frac{w}{2} F_{xfl} \cos \delta + aF_{yfl} \cos \delta + \frac{w}{2} F_{yfl} \sin \delta + aF_{xfr} \sin \delta + \frac{w}{2} F_{xfr} \cos \delta + aF_{yfr} \cos \delta - \frac{w}{2} F_{yfr} \sin \delta - \frac{w}{2} F_{xrl} - bF_{yrl} - bF_{yrr} + \frac{w}{2} F_{xrr} = I_z \ddot{\psi} \tag{3}$$

The dynamics for the sprung mass vertical motion is

$$\begin{aligned}
 & K_{sfl}(Z_{ufl} - Z_s + a\theta - 0.5w\phi) \\
 & + C_{sfl}(\dot{Z}_{ufl} - \dot{Z}_s + a\dot{\theta} - 0.5w\dot{\phi}) \\
 & + K_{sfr}(Z_{ufr} - Z_s + a\theta + 0.5w\phi) \\
 & + C_{sfr}(\dot{Z}_{ufr} - \dot{Z}_s + a\dot{\theta} + 0.5w\dot{\phi}) \\
 & + K_{srl}(Z_{url} - Z_s - b\theta - 0.5w\phi) \\
 & + C_{srl}(\dot{Z}_{url} - \dot{Z}_s - b\dot{\theta} - 0.5w\dot{\phi}) \\
 & + K_{srr}(Z_{urr} - Z_s - b\theta + 0.5w\phi) \\
 & + C_{srr}(\dot{Z}_{urr} - \dot{Z}_s - b\dot{\theta} + 0.5w\dot{\phi}) \\
 & = m_s(\ddot{Z}_s - V_x\dot{\theta} + V_y\dot{\phi})
 \end{aligned} \tag{4}$$

The dynamics for the sprung mass pitch equation of motion is given by

$$\begin{aligned}
 & b[K_{srl}(Z_{url} - Z_s - b\theta - 0.5w\phi) \\
 & + C_{srl}(\dot{Z}_{url} - \dot{Z}_s - b\dot{\theta} - 0.5w\dot{\phi}) \\
 & + K_{srr}(Z_{urr} - Z_s - b\theta + 0.5w\phi) \\
 & + C_{srr}(\dot{Z}_{urr} - \dot{Z}_s - b\dot{\theta} + 0.5w\dot{\phi})] \\
 & - a[K_{sfl}(Z_{ufl} - Z_s + a\theta - 0.5w\phi) \\
 & + C_{sfl}(\dot{Z}_{ufl} - \dot{Z}_s + a\dot{\theta} - 0.5w\dot{\phi}) \\
 & + K_{sfr}(Z_{ufr} - Z_s + a\theta + 0.5w\phi) \\
 & + C_{sfr}(\dot{Z}_{ufr} - \dot{Z}_s + a\dot{\theta} + 0.5w\dot{\phi})] = I_y\ddot{\theta}
 \end{aligned} \tag{5}$$

The dynamics for the sprung mass roll equation of motion is given

$$\begin{aligned}
 & \frac{w}{2}[K_{sfl}(Z_{ufl} - Z_s + a\theta - 0.5w\phi) \\
 & + C_{sfl}(\dot{Z}_{ufl} - \dot{Z}_s + a\dot{\theta} - 0.5w\dot{\phi}) \\
 & - K_{sfr}(Z_{ufr} - Z_s + a\theta + 0.5w\phi) \\
 & - C_{sfr}(\dot{Z}_{ufr} - \dot{Z}_s + a\dot{\theta} + 0.5w\dot{\phi}) \\
 & + K_{srl}(Z_{url} - Z_s - b\theta - 0.5w\phi) \\
 & + C_{srl}(\dot{Z}_{url} - \dot{Z}_s - b\dot{\theta} - 0.5w\dot{\phi}) \\
 & - K_{srr}(Z_{urr} - Z_s - b\theta + 0.5w\phi) \\
 & - C_{srr}(\dot{Z}_{urr} - \dot{Z}_s - b\dot{\theta} + 0.5w\dot{\phi})] \\
 & + h(F_{yfl} + F_{yfr} + F_{yrl} + F_{yrr}) = I_x\ddot{\phi}
 \end{aligned} \tag{6}$$

Fig. 3(a) presents the suspension unit for the front left corner of the sprung mass.  $Z_{sij}$ ,  $Z_{uij}$ , and  $Z_{rij}$  are vertical displacement of the sprung mass corner, vertical displacement of the unsprung mass, and road input vertical profile respectively.  $K_{sij}$ ,  $C_{sij}$ , and  $K_{tij}$  are suspension spring stiffness, damping coefficient, and tire stiffness respectively. The resultant force at each unsprung mass is determined from the summation of the spring, damper and tire forces acting on the unsprung mass. The dynamics of the unsprung mass vertical motion for front left, front right, rear left, and rear right unsprung mass are given in equation (7) to (10) respectively.

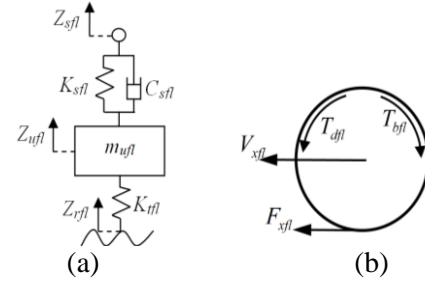


Fig. 3. Wheel dynamics model; (a) suspension model (b) wheel rotational model

$$\begin{aligned}
 & K_{tfl}(Z_{rfl} - Z_{ufl}) - K_{sfl}(Z_{ufl} - Z_s + a\theta - 0.5w\phi) \\
 & - C_{sfl}(\dot{Z}_{ufl} - \dot{Z}_s + a\dot{\theta} - 0.5w\dot{\phi}) = m_{ufl}\ddot{Z}_{ufl}
 \end{aligned} \tag{7}$$

$$\begin{aligned}
 & K_{tfr}(Z_{rfr} - Z_{ufr}) - K_{sfr}(Z_{ufr} - Z_s + a\theta + 0.5w\phi) \\
 & - C_{sfr}(\dot{Z}_{ufr} - \dot{Z}_s + a\dot{\theta} + 0.5w\dot{\phi}) = m_{ufr}\ddot{Z}_{ufr}
 \end{aligned} \tag{8}$$

$$\begin{aligned}
 & K_{trl}(Z_{rrl} - Z_{url}) - K_{srl}(Z_{url} - Z_s - b\theta - 0.5w\phi) \\
 & - C_{srl}(\dot{Z}_{url} - \dot{Z}_s - b\dot{\theta} - 0.5w\dot{\phi}) = m_{url}\ddot{Z}_{url}
 \end{aligned} \tag{9}$$

$$\begin{aligned}
 & K_{trr}(Z_{rrr} - Z_{urr}) - K_{srr}(Z_{urr} - Z_s - b\theta + 0.5w\phi) \\
 & - C_{srr}(\dot{Z}_{urr} - \dot{Z}_s - b\dot{\theta} + 0.5w\dot{\phi}) = m_{urr}\ddot{Z}_{urr}
 \end{aligned} \tag{10}$$

As shown in Fig. 3(b), the resultant torque on the wheel can be obtained by summing the driving torque, braking torque and moment due to the longitudinal force. The dynamics of the wheel spin for each wheel are as in equation (11) to (14). The effective rolling radius, wheel rotation moment of inertia, and the angular wheel velocity are indicated by  $R$ ,  $I_w$ , and  $\omega_{ij}$  respectively.

$$T_{dfl} - T_{bfl} - F_{xfl}R = I_w\dot{\omega}_{fl} \tag{11}$$

$$T_{dfr} - T_{bfr} - F_{xfr}R = I_w\dot{\omega}_{fr} \tag{12}$$

$$T_{drl} - T_{brl} - F_{xrl}R = I_w\dot{\omega}_{rl} \tag{13}$$

$$T_{drr} - T_{brr} - F_{xrr}R = I_w\dot{\omega}_{rr} \tag{14}$$

There are different tire models used by researchers in order to compute the longitudinal and lateral tire forces. Some of the tire models that can be found in literature are Magic Formula, Dugoff, and Calspan. In this paper, the tire model is based on the look up table method as presented in Fig. 4. The inputs to the tire model are the tire normal load and slip angle and the output of this model is the tire lateral force. The nonlinear tire model in Fig. 4 gives a more realistic behavior of the vehicle since it is modeled based on the tire test data.

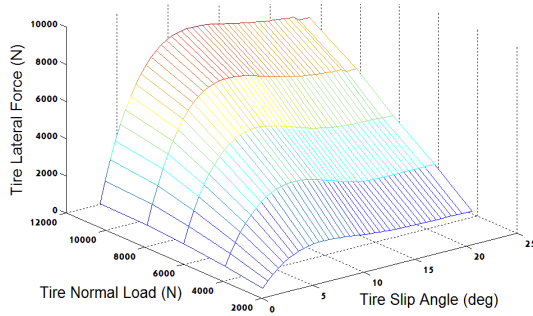


Fig. 4. Tire lateral force depending on tire normal load and slip angle

**2.3 Vehicle Subsystems Interaction**

The vehicle model subsystems interactions in Matlab/SIMULINK are demonstrated in Fig. 5. The suspension model consists of the sprung mass vertical, pitch, and roll motions and each unsprung mass vertical motion. The tire normal load subsystem computes the vertical reaction force at each tire. The tire model subsystem determines the longitudinal tire force which is a function of longitudinal slip ratio and tire normal load and lateral tire force which depends on the tire slip angle and normal load. The handling model subsystem is made of the vehicle longitudinal, lateral, and yaw motions and each wheel rotational motion. The input to the handling model is the steering angle, driving torque or braking torque, and the longitudinal and lateral tire forces.

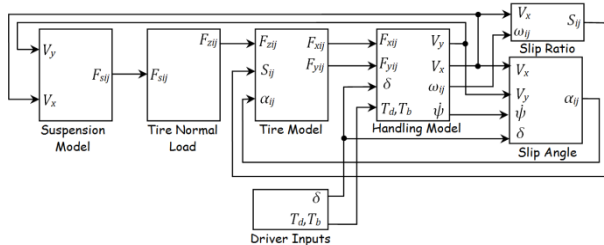


Fig. 5. Interaction between vehicle subsystems

**2.4 Validation of Vehicle Model**

The vehicle model is validated with CarSim software double lane change maneuver. The reason choosing CarSim for vehicle model validation purpose is because the performance of this software in predicting the dynamic behavior of the vehicle is very close to the responses obtained from real world testing. CarSim is proven to be accurately representing the dynamic behavior of the vehicle and it is extensively validated with experimental testing. For double lane change maneuver, the simulation was done in CarSim at a constant velocity of 80 km/h using a D-class SUV vehicle parameters as shown in Table 1. The input the CarSim for this test is the vehicle desired trajectory in which a driver model is used to generate the

steering wheel angle input based on vehicle trajectory given. Since the vehicle model used in this paper did not incorporate a driver model, the steering wheel angle which is the input to the vehicle model was obtained from CarSim software.

Table 1. Sport utility vehicle parameters

Parameter	Value
Sprung mass, $m_s$ (kg)	1429
Front unsprung mass, $m_{ufl}, m_{ufr}$ (kg)	40
Rear unsprung mass, $m_{urt}, m_{urr}$ (kg)	40
Sprung mass roll inertia, $I_r$ ( $\text{kgm}^2$ )	377
Sprung mass pitch inertia, $I_p$ ( $\text{kgm}^2$ )	1765
Sprung mass yaw inertia, $J_z$ ( $\text{kgm}^2$ )	1765
Sprung mass C.G height, $h$ (m)	0.67
Sprung mass C.G to front axle distance, $a$ (m)	1.05
Sprung mass C.G to rear axle distance, $b$ (m)	1.57
Track width, $w$ (m)	1.57
Front suspension stiffness, $K_{sfl}, K_{sfr}$ ( $\text{Nm}^{-1}$ )	34000
Rear suspension stiffness, $K_{srl}, K_{srr}$ ( $\text{Nm}^{-1}$ )	34000
Front suspension damping coefficient, $C_{sfl}, C_{sfr}$ ( $\text{Nsm}^{-1}$ )	2400
Rear suspension damping coefficient, $C_{srl}, C_{srr}$ ( $\text{Nsm}^{-1}$ )	2400
Tire stiffness, $K_{tfl}, K_{tfr}, K_{trl}, K_{trr}$ ( $\text{Nm}^{-1}$ )	230000
Effective rolling radius, $R$ (m)	0.36

**3 Active Roll Control Strategy**

The proposed active roll control strategy the comprise of feedback fuzzy logic control and feedforward fuzzy logic control is presented in Fig. 6. For the feedforward fuzzy logic control, road steering wheel angle and the longitudinal vehicle velocity were chosen as the inputs and the counter roll moment was selected as the output. The inputs for the feedback fuzzy logic control were the roll angle error and its error rate and the output is the counter roll moment. The roll angle error is defined as the difference between the desired roll angle,  $\phi_d$  and actual roll angle,  $\phi_a$  as in equation (15). The resultant counter roll,  $M_\phi$  which the summation of the counter roll moment by the feedforward fuzzy control,  $M_{\phi ff}$  and counter roll moment due to feedback fuzzy control,  $M_{\phi fb}$  is given in equation (16).

$$e_\phi = \phi_d - \phi_a \tag{15}$$

$$M_\phi = M_{\phi ff} + M_{\phi fb} \tag{16}$$

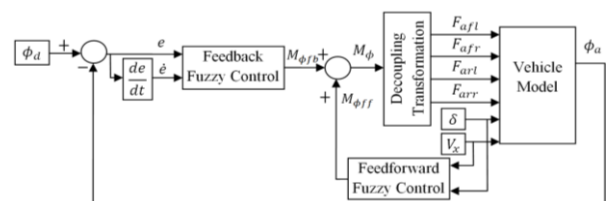


Fig. 6. Combination of feedback and feedforward roll control strategy

### 3.1 Feedforward Fuzzy Logic Control

Feedforward fuzzy control calculates the counter roll moment based on the road wheel steering angle and longitudinal vehicle velocity [13]. As presented in Figs. 7 to 9, seven Gaussian membership functions were selected for road steering wheel angle, five Gaussian membership functions for the longitudinal vehicle velocity error rate and seven Gaussian memberships functions for the counter roll moment. The Gaussian membership function was used due to their smooth mapping property. The seven variables for the road steering input and counter roll moment are negative large (NL), negative medium (NM), negative small (NS), zero (Z), positive small (PS), positive medium (PM), and positive large (PL). The five variables for the longitudinal vehicle velocity are very slow (VS), slow (S), normal (N), fast (F), and very fast (VF). The universe of discourse for the inputs was set based on their operating range. The counter roll moment from feedforward fuzzy control is obtained with a scaling factor of 5000 as shown in equation (17).

$$M_{\hat{\phi}ff} = 5000\hat{M}_{\hat{\phi}ff} \quad (17)$$

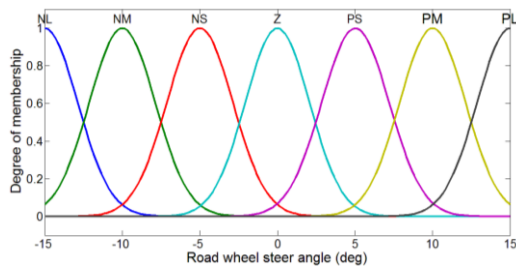


Fig. 7. Road steering wheel angle membership functions for feedforward fuzzy control

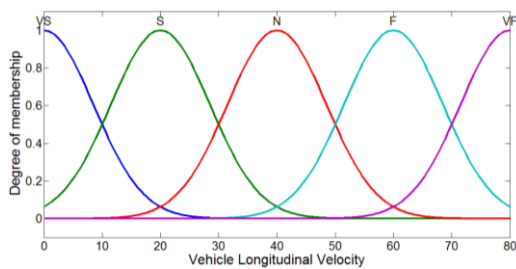


Fig. 8. Longitudinal vehicle velocity membership functions for feedforward fuzzy control

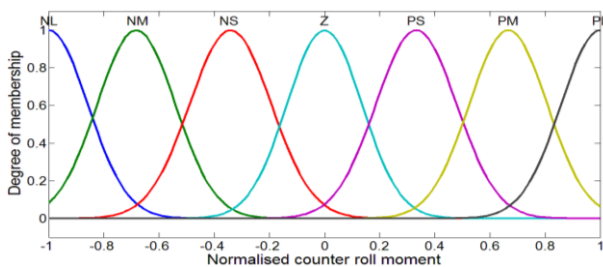


Fig. 9. Counter roll moment membership functions for feedforward fuzzy control

Table 2. Rule table for feedforward fuzzy control

Velocity \ Steer	NL	NM	NS	Z	PS	PM	PL
VS	Z	Z	Z	Z	Z	Z	Z
S	NM	NM	NM	Z	PM	PM	PM
N	NL	NM	NM	Z	PM	PM	PL
F	NL	NL	NL	Z	PL	PL	PL
VF	NL	NL	NL	Z	PL	PL	PL

### 3.2 Feedback Fuzzy Logic Control

For feedback fuzzy control, each roll angle error, roll angle error rate and counter roll moment has five Gaussian membership functions. The five variables for the roll angle error, roll angle error rate and counter roll moment are negative medium (NM), negative small (NS), zero (Z), positive small (PS), and positive medium (PM). The membership functions for roll angle error, roll angle error rate, and counter roll moment are depicted in Figs. 10, 11, and 12 respectively. The universe of discourse for the counter roll moment was normalized in the range [-1 1]. The counter roll moment was scaled by heuristic method to obtain the best scaling factor. The final counter roll moment output with a 5000 scaling factor is as in equation (18).

$$M_{\hat{\phi}fb} = 5000\hat{M}_{\hat{\phi}fb} \quad (18)$$

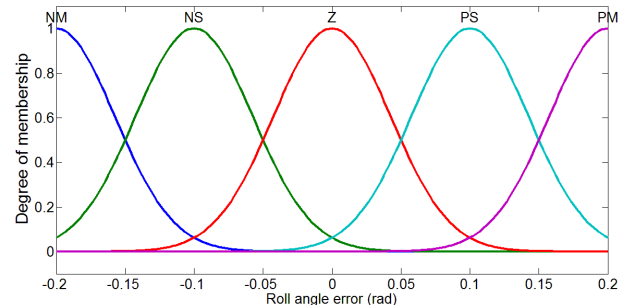


Fig. 10. Roll angle error membership functions for feedback fuzzy control

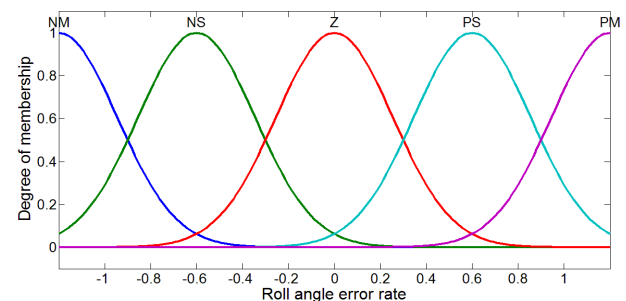


Fig. 11. Roll angle error rate membership functions for feedback fuzzy control

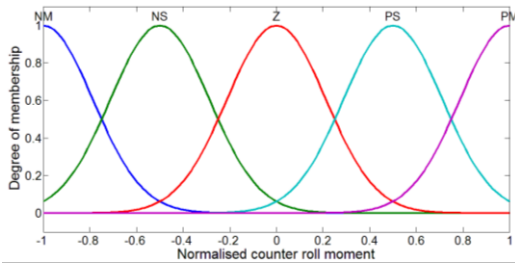


Fig. 12. Normalised counter roll moment membership functions for feedback fuzzy control

Table 2. Rule table for feedback fuzzy logic control

Error rate \ Error	NM	NS	Z	PS	PM
NM	NM	NM	NM	PM	PM
NS	NM	NS	NS	PS	PM
Z	NM	NS	Z	PS	PM
PS	NM	NS	PS	PS	PM
PM	NM	NM	PM	PM	PM

### 3.3 Active Suspension

Active suspension as presented in Fig. 13 is used to reduce the vehicle roll motion by providing counter roll moment. During cornering, lateral force acts at the body center of gravity. Roll moment is created by the lateral force. The controller determines the actuator forces required to create a counter roll moment to reduce vehicle roll angle. There are four actuator inputs  $F_{afl}$ ,  $F_{afr}$ ,  $F_{arl}$ , and  $F_{arr}$  which are the actuator forces located at the corners of the vehicle body.

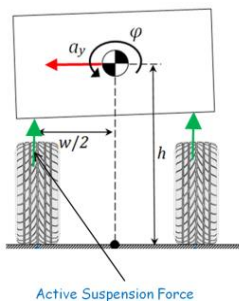


Fig.13. Active suspension

The counter roll moment due to the actuator forces is given in equation (19).

$$M_{\phi} = 0.5w(F_{afl} - F_{afr} + F_{arl} - F_{arr}) \tag{19}$$

By matrix manipulation, the actuator force at each corner is as in equation (20).

$$\begin{bmatrix} F_{afl} \\ F_{afr} \\ F_{arl} \\ F_{arr} \end{bmatrix} = \begin{bmatrix} 1 \\ 2w \\ 1 \\ -2w \\ 1 \\ 2w \\ 1 \\ -2w \end{bmatrix} [M_{\phi}] \tag{20}$$

## 4 Results and discussion

### 4.1 Validation of vehicle model with CarSim software

The vehicle model was validated with CarSim for double lane change maneuver at 80 km/h. As in Fig. 14, the steering angle inputs for the front wheel of vehicle model were taken from CarSim. The roll angle, and roll rate responses are depicted in Figs. 15 and 16 respectively. For roll angle and roll rate responses, the trend of both vehicle model and CarSim are identical with small differences in magnitude compared to CarSim. The main contributing factor to the difference in magnitude between the vehicle model and CarSim responses are the modeling simplification in the development of the vehicle model particularly in modeling the suspension system. CarSim is a multibody software, whereas vehicle model is developed analytically.

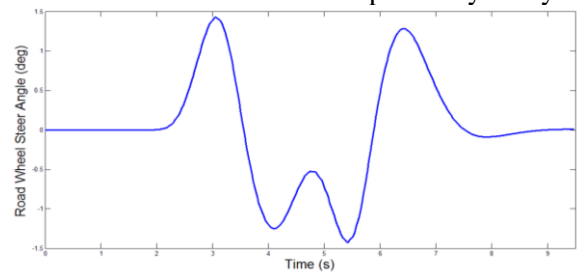


Fig. 14. Road wheel steering angle for double lane change at 80 km/h

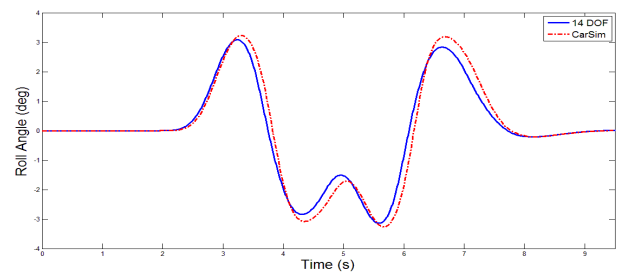


Fig. 15. Roll angle response for double lane change at 80 km/h

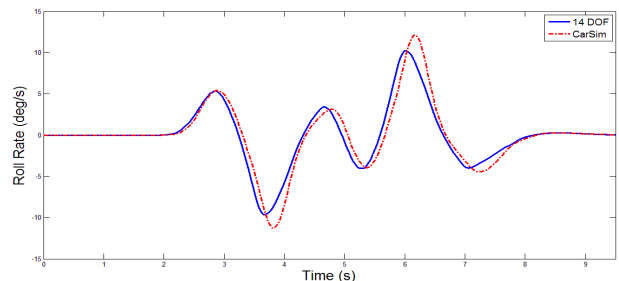


Fig. 16. Roll rate response for double lane change at 80 km/h

### 4.2 Performance evaluation for fishhook maneuver

The performance of proposed active roll control strategy in reducing the roll angle and roll rate for fishhook maneuver at 64.4 km/h are demonstrated in Figs. 17 and 18 respectively. The root mean square values of the passive system, active roll control using feedforward fuzzy, and active roll control using a combination of feedback and feedforward fuzzy for fishhook maneuver at 64.4 km/h are tabulated in Table 4. The feedforward fuzzy control which takes the road steering wheel angle and vehicle longitudinal velocity as the inputs greatly reduces the risk to rollover by reducing the roll angle and roll rate. Additional improvement is provided by the combination of feedforward and feedback fuzzy control in lowering the value of the both roll angle and roll rate.

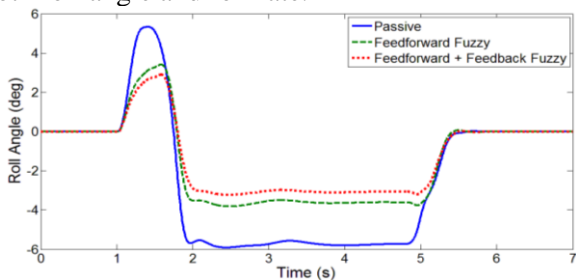


Fig.17. Roll angle response for fishhook at 64.4km/h

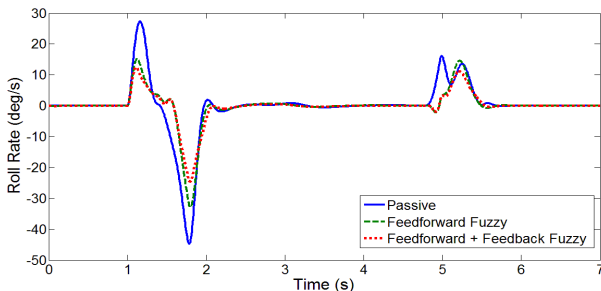


Fig. 18. Roll rate response for fishhook at 64.4 km/h

Table 4. RMS for fishhook test at 64.4 km/h

Performance criteria	Passive	Feedforward fuzzy	Feedback & feedforward fuzzy
Roll angle	4.09	2.62	2.22
Roll rate	8.50	5.79	4.61

### 4.3 Performance evaluation for step steer test

For 140 degrees step steer at 60 km/h maneuver, it can be seen in Fig. 19 that the roll angle is extensively reduced and the overshoot during the transient state is dampen during the maneuver. Also, the roll rate of the vehicle is improved by the feedforward fuzzy control as depicted in Fig. 20. The combination of the feedforward and feedback fuzzy offers better performance in reducing the roll angle and roll rate for the step steer maneuver compared to roll control based on only feedforward

fuzzy. The root mean square of these responses is presented in Table 5.

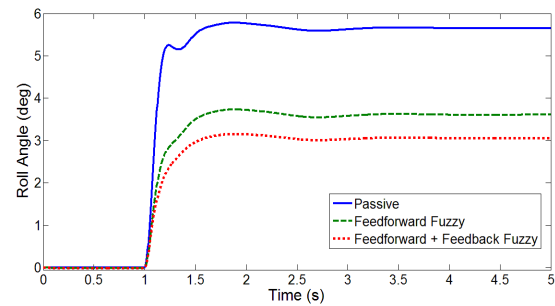


Fig. 19. Roll angle response for 140 degrees step steer test at 60 km/h

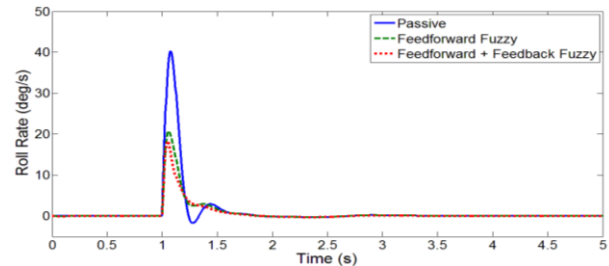


Fig. 20. Roll rate response for 140 degrees step steer test at 60 km/h

Table 5. RMS for 140 deg step steer test at 60 km/h

Performance criteria	Passive	Feedforward fuzzy	Feedback & feedforward fuzzy
Roll angle	4.95	3.14	2.66
Roll rate	5.65	3.00	2.47

### 4.4 Performance evaluation for double lane change

For double lane change maneuver simulation at 80 km/h, the improvement by feedforward fuzzy and combination of both feedforward and feedback fuzzy are not as good as for fishhook and step steer maneuvers because double lane change maneuver does not excite the roll behavior of the vehicle as much as the other two maneuvers. The roll angle and roll rate for double lane change maneuver are depicted in Figs. 21 and 22 respectively.

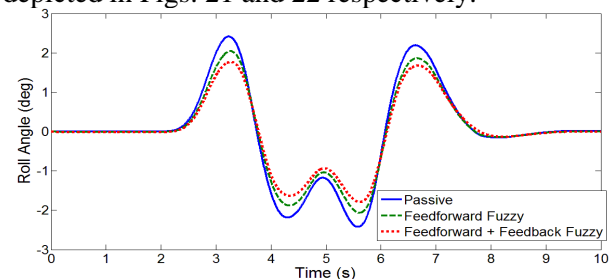


Fig. 21. Roll rate response for 140 degrees step steer test at 60 km/h

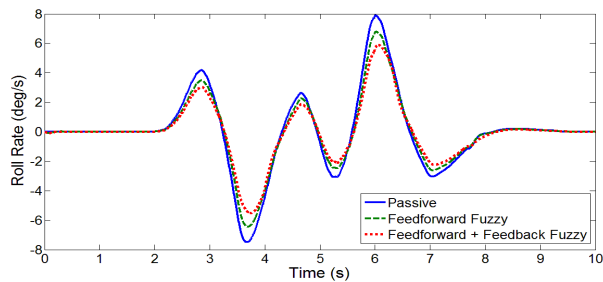


Fig. 22. Roll rate response for 140 degrees step steer test at 60km/h

The root mean square values for the passive system, active roll control using feedforward fuzzy, and active roll control using combination of feedback and feedforward fuzzy for double lane change maneuver at 80 km/h are tabulated in Table 6.

Table 6. RMS for double lane change maneuver at 80 km/h

Performance criteria	Passive	Feedforward fuzzy	Feedback & feedforward fuzzy
Roll angle	1.18	1.01	0.89
Roll rate	2.66	2.27	1.98

## 5 Conclusion

A 14 DOF vehicle model was developed and validated with CarSim software. A fuzzy based active suspension control scheme was designed in Matlab/SIMULINK environment. The performance of the active roll control using active suspension was evaluated for fishhook, step steer, and double lane change manoeuvres. The feedforward fuzzy control greatly reduces vehicle roll angle. The addition of feedback fuzzy improves further the roll behaviour. The reduction in the roll angle signifies that there is improvement in preventing rollover under severe driving conditions.

## Acknowledgement

The authors wish to thank the Universiti Teknikal Malaysia Melaka (UTeM) for providing the research grant and facilities. This research is supported using a research grant, PJP/2012/FKM(1C)/S01006.

## References:

[1] Rajamani, R. (2012). Vehicle dynamics and control (2nd Ed.). New York: Springer.  
 [2] Rakheja, S. & Pichè, A. (1990). Development of Directional Stability Criteria for an Early Warning Safety Device. SAE Paper No.902265.  
 [3] Dahlberg, E. (2000). A Method Determining the Dynamic Rollover Threshold of

Commercial Vehicles. SAE Paper No. 2000-01-3492.

- [4] Chen, B. & Peng, H. (1999). Rollover Warning for Articulated Vehicles Based on a Time-to-rollover Metric. Proceedings of ASME International Mechanical Engineering Congress and Exposition. Nashville, TN.  
 [5] Hudha, K., Kadir, Z., Said, M. R., & Jamaluddin, H. (2008). Modeling, Validation, and Roll Moment Rejection Control of Pneumatically Actuated Active Roll Control for Improving Vehicle Lateral Dynamics Performance. International Journal Engineering System Modelling and Simulation. 1(2), 122-136.  
 [6] Sornioti, A. & D'Alfio, N. (2007). Vehicle Dynamics Simulation to Develop an Active Roll Control System. SAE paper No. 2007-01-0828.  
 [7] Sampson, D. J. M. & Cebon, D. (2003). Active Roll Control of Single Unit Heavy Road Vehicles. Vehicle System Dynamics. 40(4), 229-270.  
 [8] Wielenga, T. J. (1999). Method for Reducing On-Road Rollovers: Anti-Rollover Braking. SAE paper No. 1999-01-0123.  
 [9] Solmaz, S., Corless, M., & Shorten, R. (2006). A Methodology for the Design of Robust Rollover Prevention Controllers for Automotive Vehicles: Part 1-Differential Braking. Proceedings of the Conference on Decision and Control. San Diego.  
 [10] Shim, T., Toomey, D., Ghike, C., & Sardar, H. M. (2008). Vehicle Rollover Recovery using Active Steering/Wheel Torque Control. International Journal Vehicle Design. 46(1), 51-71.  
 [11] Ackermann, J., Odenthal, D., & Bunte, T. (1999). Advantages of Active Steering for Vehicle Dynamics Control. 32nd International Symposium on Automotive Technology and Automation, (pp. 263-270). Vienna.  
 [12] March, C. & Shim, T. (2007). Integrated Control of Suspension and Front Steering To Enhance Vehicle Handling. Proceedings of the Institution of Mechanical Engineers, Part D: Journal of Automobile Engineering. 221(4), 377-391.  
 [13] Khajavi, M. N., Hemmati, V., & Shouredeli, S. (2009). A Novel Approach to Enhance Roll Stability of SUVs by a Fuzzy Logic Controller. World Academy of Science, Engineering and Technology, 49.